The origin of coupled chloride and proton transport in a Cl^-/H^+ antiporter

Sangyun Lee, Heather B. Mayes, Jessica M. J. Swanson, and Gregory A. Voth*

Department of Chemistry, James Franck Institute, Institute for Biophysical Dynamics, and Computation Institute, University of Chicago

Introduction

ClC-ec1 is a member of the chloride channels and transporters (ClC) family, which pumps H^+ against its concentration gradient through the membrane using Cl^- gradient in the opposite direction, or vice versa. We have studied **the proton transport mechanism** by 1) developing **multi-scale reactive molecular dynamics (MS-RMD) model** to explicitly simulate the protonation/deprotonation reaction of amino acids and the diffusion of the excess proton through internal water chain, and 2) calculating **the free energy profile of a proton** along its transport pathway in WT and its E148A mutant of the protein. Our simulation results suggested the essential mechanism of the Cl^-/H^+ coupling and the rate limiting step for proton transport in WT, and explained how proton transport is blocked in E148A mutant.

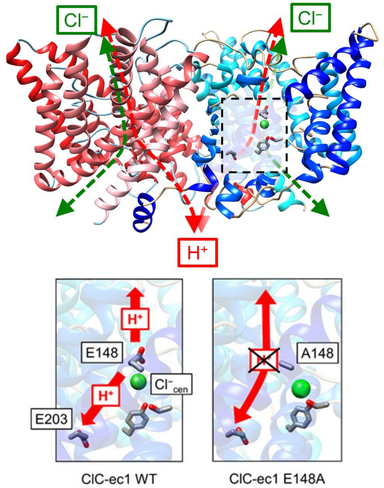

(Top) Overview of the structure of ClC-ec1 and transport pathways for Cl^- (green) and H^+ (red). The central region is highlighted in the black box.
(Bottom) Proton transport (PT) mechanism in WT and its E148A mutant of ClC-ec1. Deprotonation of E148 is the rate-limiting step in PT in both outflux and influx directions. PT through A148 is blocked in E148A mutant.

Method

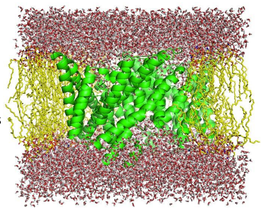

Simulation System

- A ClC-ec1 dimer
- 168 of POPE lipids
- ~11k of water molecules
- ~17 Cl^- ions.
- 66 k atoms in total.
- Charmm22 force field

Proton Transport

1) The MS-RMD models for the protonation/deprotonation of E148 and E203 were parameterized by using adaptive force matching to the reference QM/MM data from ~500 configurations sampled at protonated and deprotonated states for each residue.
2) The Metadynamics simulation was executed to sample a curvilinear pathway through irregular shaped internal protein structure for proton transport at two regions: from E203 to E148, and from E148 to the extracellular solution.
3) The potential of mean force (PMF) for proton transport in WT and two other mutants were calculated by doing the replica exchange umbrella sampling (REUS) along the curvilinear pathway.

Results

MS-RMD reactive Force-Field Modeling

- The model parameters were fit to QM/MM reference forces using FitEVB algorithm.
- MS-RMD models reproduced the PMF of the reference QM/MM Hamiltonian (DFT-BLYP(D3)/TZV2P) for PT in the central region.
- The MS-EVB will extend the limit of sampling time in QM/MM MD for typical biological systems from picoseconds to nanoseconds.

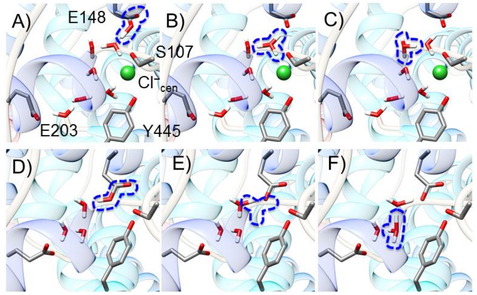

Excess proton is delocalized into a Glutamate residue and surrounding water molecules. Representative configurations of a set of MS-RMD states with different bonding topologies for the same atomic coordinates, when Cl^-_{cen} is present (A-C) or absent (D-F).

PMFs of PT through central region of ClC-ec1 with (A) Cl^-_{cen} present and (B) absent, as calculated with MS-RMD (blue) and QM/MM (red).

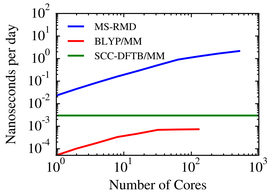

Scaling plot for the simulation speed with different MD simulation methods. The MS-RMD method is 2-3 orders of magnitude faster than other QM/MM methods, while more favorable scaling properties over processors.

Hydration of the central region is a rare event.

- No water molecules have been found in the X-ray crystal structure, which can mediate PT through the central region.
- The formation of water wire structure in the central region is a rare event in the MD simulation.

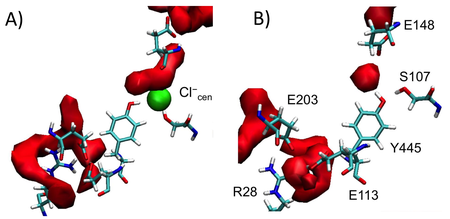

The water density map (red) in the central region, averaged over 50 ns trajectories of classical MD simulations, with Cl^-_{cen} present (A) and absent (B). The water wire between E148 and E203 is disconnected most of the time in both cases.

Collective variables (CV) in the PMFs of PT and coupled hydration in the central region.

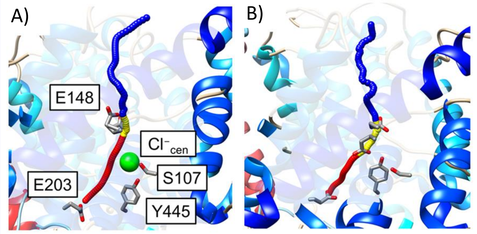

CV1: The curvilinear PT pathway calculated from MetaD simulation.

The PT pathway with Cl^-_{cen} present (A) and absent (B) Red: PT from E203 to E148 (central region). Yellow: Rotation of E148. Blue: PT from E148 to the extracellular solution.

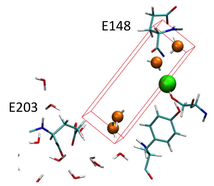

CV2: The water density of the central region.

The effective number of water molecules (orange spheres) in the red box.

Proton transport from E203 to E148

- 2D PMFs show that PT from E203 to E148 is coupled with the hydration of the central region.

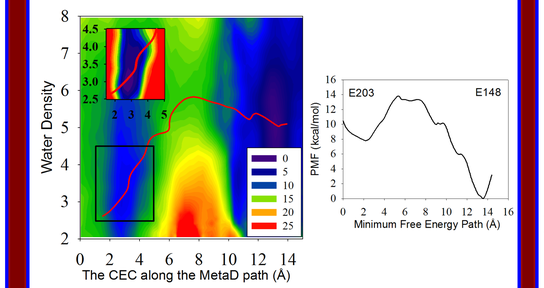

(left) The 2D PMF of WT with Cl^-_{cen} present. The red line on the 2D PMF represents the minimum free energy path between two local energy minima.
(right) The 1D PMF calculated along that minimum free energy path.

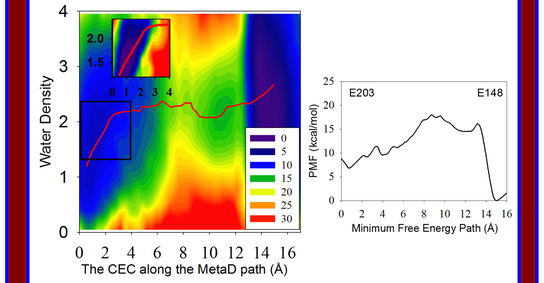

(left) The 2D PMF of WT with Cl^-_{cen} absent.
(right) The 1D PMF trace along the minimum free energy path.

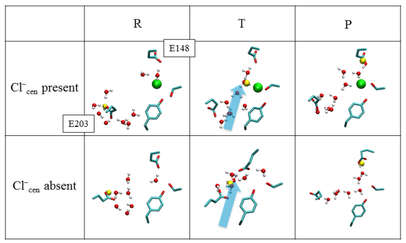

Representative configurations of the central region at the reactant (R), transition (T), and product states (P) in the 2D PMFs with Cl^-_{cen} present and absent.

Rotation of E148, and proton transport from E148 to the solution

- 1D PMFs was calculated for two-step processes: 1) the rotation of protonated E148, and 2) E148 deprotonation to the extracellular solution.

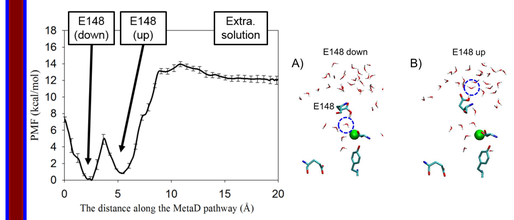

(left) The PMF for a two-step PT process with Cl^-_{cen} present, from protonated E148 in the down conformation to the extracellular solution.
(right) Representative configurations in the PMF for E148 down (A) and up conformations (B).

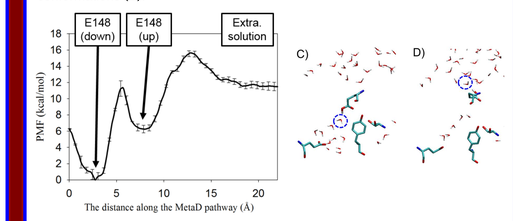

(left) The PMF with Cl^-_{cen} absent.
(right) Representative configurations for E148 down (C) and up (D).

- The p*Ka* of E148 calculated from the PMF (6.9) was comparable to the experimental value. (6.2)

Proton transport in E148A mutant

- Experiment shows that E148A mutant cannot transport protons, but it allows pH-independent Cl^- flux.
- The PMF shows that PT past A148 is effectively blocked, regardless of the presence of Cl^-_{cen}, in agreement with experimental findings.

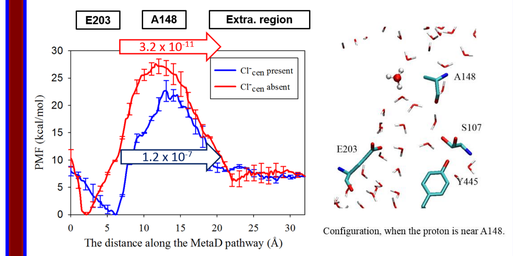

Configuration, when the proton is near A148.

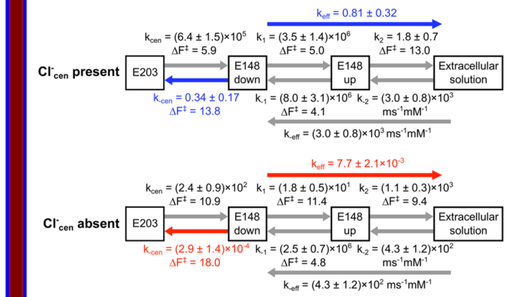

The rate constant and the free energy barriers of the intermediate steps in ClC-ec1 WT with Cl^-_{cen} present (top) or absent (bottom).
The gray arrows represent fast (non-limiting) steps, blue represent rate-limiting steps, and red represent steps that effectively block PT.
The experimental value for the turnover rate for PT is 1.0 ms^{-1}.

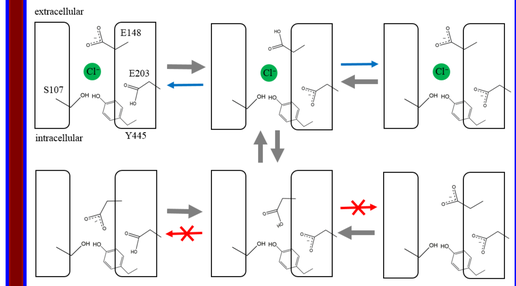

Schematic representation of the PT mechanism in ClC-ec1 WT with Cl^-_{cen} present (top) or absent (bottom). PT with Cl^-_{cen} absent is blocked at the second step until a new Cl^- enters the central site, while E148 is protonated.

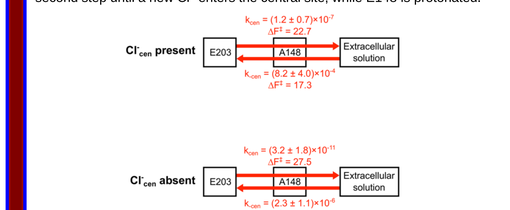

The rate constant and the free energy barriers in ClC-ec1 E148A mutant. PT is blocked in both outflux and influx directions, regardless of the presence of Cl^-_{cen}.

Conclusions

- MS-RMD enables to explicitly simulate the proton delocalized in surrounding protonation sites, and the protonation/deprotonation of amino acids.
- PT from E203 to E148 induces the hydration of the central region.
- The rate-limiting step for proton transport is the deprotonation of E148, which is facilitated by the presence of Cl^-_{cen}.
- Conversely, in the absence of Cl^-_{cen}, E148 favors the "down" conformation, which results in a much higher cumulative rotation and deprotonation barrier that effectively blocks PT to the extracellular solution.
- PT in E148A is blocked whether or not Cl^-_{cen} is present.

Acknowledgement

This investigation was supported by the University of Chicago Research Computing Center (RCC) and the National Institutes of Health (NIH grant R01 GM053148).